

Dynamics of Kinks: Nucleation, Diffusion and Annihilation

Salman Habib[†] and Grant Lythe^{*}

[†]*T-8, Theoretical Division, MS B285, Los Alamos National Laboratory, Los Alamos, New Mexico 87545*

^{*}*Center for Nonlinear Studies, Los Alamos National Laboratory, Los Alamos, New Mexico 87545*

(April 11, 2018)

We investigate the nucleation, annihilation, and dynamics of kinks in a classical (1+1)-dimensional ϕ^4 field theory at finite temperature. From large scale Langevin simulations, we establish that the nucleation rate is proportional to the square of the equilibrium density of kinks. We identify *two* annihilation time scales: one due to kink-antikink pair recombination after nucleation, the other from non-recombinant annihilation. We introduce a mesoscopic model of diffusing kinks based on “paired” and “survivor” kinks/antikinks. Analytical predictions for the dynamical time scales, as well as the corresponding length scales, are in good agreement with the simulations.

PACS numbers: 05.20.-y, 11.10.-z, 63.75.+z, 64.60.Cn

Many extended systems have localized coherent structures that maintain their identity as they move, interact and are buffeted by local fluctuations. The statistical mechanics of these objects has diverse applications, *e.g.*, in condensed matter physics [1], biology [2], and particle physics [3]. The model to be studied here is a kink-bearing ϕ^4 field theory in (1 + 1) dimensions, popular because its properties are representative of those found in many applications. Static equilibrium quantities of this theory, such as the kink density and spatial correlation functions, are now well understood and recent work has shown that theory and simulations are in good agreement [4–6]. However, dynamical processes, both close to and far out of equilibrium, are much less well understood. Questions include: What is the nucleation rate of kink-antikink pairs? How is an equilibrium population maintained? How do these dynamical processes depend on the temperature and damping? These questions, among others, are the subject of this Letter.

We introduce and analyze below a simple model of kink diffusion and annihilation that predicts the nucleation rate and provides a picture of the physical situation, including the existence of multiple time and length scales. We also carry out high resolution numerical simulations. As one consequence of our work, we are able to settle a recent controversy as to whether the nucleation rate of kinks in an overdamped system is proportional to $\exp(-2E_k\beta)$ [7] or $\exp(-3E_k\beta)$ [8] in favor of the first result (E_k is the kink energy and $\beta = 1/k_B T$).

We consider the dynamics of the ϕ^4 field obeying the following dimensionless Langevin equation [4]:

$$\partial_{tt}^2 \phi = \partial_{xx}^2 \phi + \phi(1 - \phi^2) - \eta \partial_t \phi + \xi(x, t), \quad (1)$$

with the fluctuation-dissipation relation enforced by $\langle \xi(x, t) \xi(x', t') \rangle = 2\eta\beta^{-1} \delta(x - x') \delta(t - t')$. We perform simulations on lattices typically of 10^6 sites, using a finite difference algorithm that has second-order convergence to the continuum [6]. Typical values of the grid spacing and time step are $\Delta x = 0.4$ and $\Delta t = 0.01$.

At zero temperature, the static kink solution centered at $x = x_0$ is $\phi_k(x) = k(x - x_0)$ where $k(x) = \tanh(x/\sqrt{2})$; the corresponding antikink solution is $\phi_a(x) = -k(x - x_0)$. Because there are only two potential minima, kinks alternate with antikinks on the spatial lattice. Imposing periodic boundary conditions constrains the number of kinks and antikinks to be equal. During the time evolution, we identify kinks and antikinks individually and follow the “lifeline” of each kink or antikink (Fig. 1).

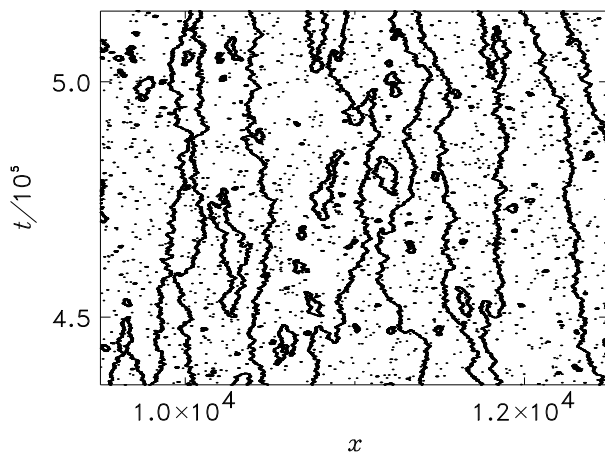


FIG. 1. Timelines of kinks and antikinks: A small space-time portion of one numerical solution is shown. Many recombination nucleation-annihilation events are barely visible, forming small closed loops. $\beta = 7$, $\eta = 1$.

Equilibrium properties of one-dimensional systems, such as the free energy density and the correlation function $\langle \phi(0)\phi(x) \rangle$, can be calculated using the transfer integral method [9]. The calculation is exact, although one typically must evaluate eigenvalues of the resulting Schrödinger equation numerically. When the on-site potential has the double-well form, as is the case here, one part of the free energy density at low temperature can be interpreted as due to kinks, forming a dilute gas with

density [9]: $\rho_k \propto \sqrt{E_k \beta} \exp(-E_k \beta)$. This WKB approximation is consistent with recent simulations at $\beta > 6$, where unambiguous identification of kinks is possible [4].

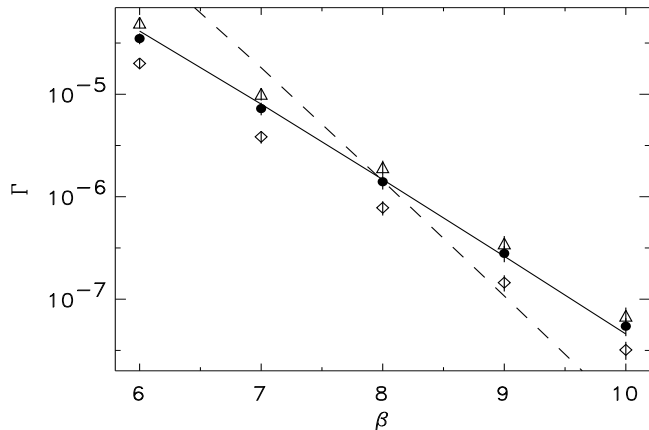


FIG. 2. Nucleation rate, measured from numerical solution of (1) with tracking of timelines. The rate, Γ , of production per unit length per unit time of kink-antikink pairs is shown versus β for three values of η : $\eta = 0.2$ (triangles), $\eta = 1$ (filled circles) and $\eta = 5$ (diamonds). The solid line is $\Gamma = \rho_k^2$ and the dashed line is the best fit to $\Gamma = a\rho_k^3$ for $\eta = 1$.

An equilibrium density of kinks is maintained by a dynamical balance of nucleation and annihilation of kink-antikink pairs (Fig. 1). The dependence of the nucleation rate Γ on temperature and damping, however, is not directly calculable from the transfer integral; nor are unambiguous results for symmetric potentials available from saddle-point calculations [10]. While analogy with the Kramers' problem suggests $\Gamma \propto \exp(-2\beta E_k)$ [11], the relationship $\Gamma \propto \exp(-3\beta E_k)$ has also been suggested [8]. Our direct counting of nucleation events establishes that their rate is proportional to the square of the equilibrium density, that is $\Gamma \propto \exp(-2\beta E_k)$ (Fig. 2). Below we show how this relation can be understood from a mesoscopic model of diffusing kinks with paired nucleation.

At equilibrium, the nucleation rate is related to the mean kink lifetime τ by $\rho_k = \Gamma\tau$. Previous attempts to evaluate Γ numerically [12,13] have proceeded by counting the number of kinks $n_k(t)$ and assuming exponential decay of $\langle n_k(t+\tau)n_k(t) \rangle$. Unfortunately this approach provides no information on the underlying processes, and yields incorrect results if kinks are not properly identified on the lattice. In particular, results that appeared to support $\Gamma \propto \exp(-3\beta E_k)$ were performed at temperatures too high for accurate computation of $\langle n_k(t+\tau)n_k(t) \rangle$ [12].

Because we identify individual nucleation events and follow individual kink lifelines, we can distinguish “paired” kinks (whose partner antikink is still alive) from “survivor” kinks (whose partner has been killed). We also distinguish and measure the contributions to the annihilation rate from the recombinant and various non-recombinant mechanisms (Fig. 3). The most fre-

quent annihilation event is recombination of a recently-nucleated pair (designated I in Fig. 3) [7]. However, the “survivor” kinks that remain after a non-recombinant annihilation event (II or III) have a longer mean lifetime.

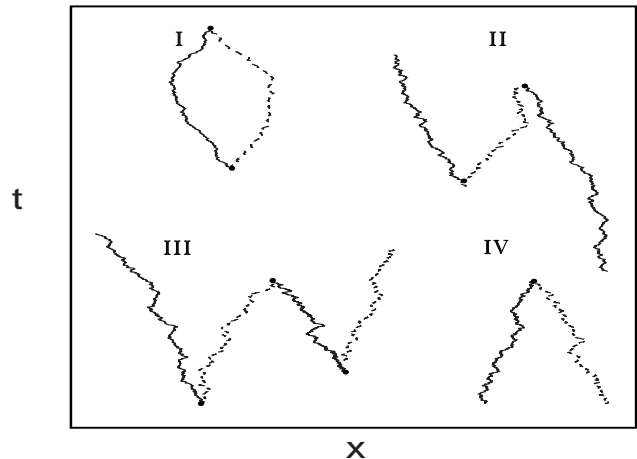


FIG. 3. The four kink-antikink annihilation processes. I: Recombination of a paired kink and antikink; II: Annihilation of a survivor with a paired kink/antikink; III Annihilation of a kink and an antikink from two neighboring nucleation sites (producing a survivor kink and antikink); IV Annihilation of two survivors.

At finite temperature, the mean-squared displacement of an isolated kink is given by $\langle \mathbf{X}_t^2 \rangle = 2Dt$. The diffusivity D can be estimated by using the zero-temperature kink as an ansatz in the equation of motion (1), yielding $D \simeq (E_k \beta \eta)^{-1}$ [14], where $E_k = \sqrt{8/9}$ for a static kink. Corrections to D , arising because of fluctuations in the kink shape, are proportional to β^{-2} and subdominant in the temperature range considered here.

Our numerical observations, in particular that kink-antikink collisions at moderate to large damping always result in annihilation, motivate us to introduce the following mesoscopic model of kink dynamics: (i) kink-antikink pairs are nucleated at random times and positions with initial separation $b \ll \rho_k^{-1}$; (ii) once born, kinks and antikinks diffuse independently with diffusivity D ; (iii) kinks and antikinks annihilate on collision. The separation between a kink and its partner performs Brownian motion with diffusivity $2D$. Thus, if only recombine annihilation (I in Fig. 3) were allowed, the time t_0 between nucleation and annihilation would have the density $\frac{d}{dt} \mathcal{P}[t_0 < t] = bt^{-\frac{3}{2}} (8\pi D)^{-\frac{1}{2}} \exp(-\frac{b^2}{8Dt})$ [15].

To analyse our model, we use the following approximation for non-recombinant annihilation: as long as both members of a pair are alive, there is a constant probability μ per unit time of a member being struck and “killed” by an outsider, *i.e.* of an event II or III. Thus, to each pair we assign a killing time t_μ , distributed according to $\mathcal{P}[t_\mu > t] = \exp(-\mu t)$. Non-recombinant annihilation happens with probability $\mathcal{P}[t_\mu < t_0] = 1 - \exp(-bt)$,

where $\nu^2 = \frac{\mu}{2D}$ [16,17]. The killing rate μ depends on the density of kinks; we estimate it as follows. A newborn pair finds itself in a domain between an existing kink and antikink of typical length $1/(2\rho_k)$. The mean time for a diffusing particle to exit the region is proportional to $(2D\rho_k^2)^{-1}$. Therefore, let

$$\mu = 2D\alpha^2\rho_k^2. \quad (2)$$

The value of the dimensionless factor was obtained from numerical measurements of length and timescales (see Figures 4 and 6 below): we estimate $\alpha \simeq 8$.

Let $R(t) = \frac{d}{dt}\mathcal{P}[\mathbf{t}_0 < t | \mathbf{t}_0 < \mathbf{t}_\mu]$. Then

$$R(t) = N(b) \exp\left(-\frac{b^2}{8Dt}\right) t^{-\frac{3}{2}} \exp(-\mu t), \quad (3)$$

where $N(b) = b(8\pi D)^{-\frac{1}{2}} \exp(\nu b)$. In Fig. 4 we plot (3) and a histogram of values of \mathbf{t}_0 obtained from a large numerical solution of (1). The behavior $R(t) \propto t^{-\frac{3}{2}}$ is characteristic of Brownian excursions [15].

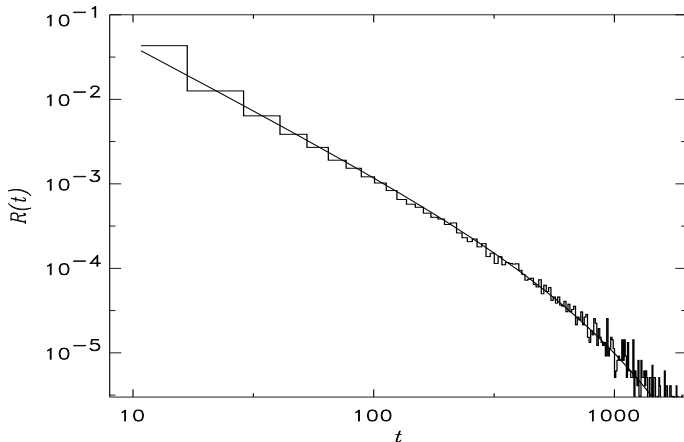


FIG. 4. Recombination time density. Only recombinant histories (I in Fig. 3) are counted. The solid line is (3). The histogram is from a simulation of (1). $\beta = 6$, $\eta = 1$.

Our mesoscopic model has two timescales [17]:

$$\tau_0 = \langle \mathbf{t}_0 | \mathbf{t}_0 < \mathbf{t}_\mu \rangle = \frac{b}{2\sqrt{\mu D}}, \quad (4)$$

$$\tau_\mu = \langle \mathbf{t}_\mu | \mathbf{t}_\mu < \mathbf{t}_0 \rangle = \frac{1}{\mu} \left(1 - \frac{\nu b}{2} \frac{1}{e^{\nu b} - 1} \right). \quad (5)$$

The mean recombination time (4) depends on b ; in contrast τ_μ has a non-zero limit for $\nu b \rightarrow 0$: $\tau_\mu \rightarrow 1/(2\mu)$. With the approximation that a “survivor” kink/antikink has the same probability per unit time, μ , of collision and death, the *mean lifetime of a kink or antikink* is given by

$$\tau = \tau_0 e^{-\nu b} + \tau_\mu (1 - e^{-\nu b}) + \frac{1}{2\mu} (1 - e^{-\nu b}). \quad (6)$$

As $\rho b \rightarrow 0$, $\tau \rightarrow (3/2)b(2\mu D)^{-1/2} = (3/4)b(\alpha D\rho)^{-1}$. In the same limit, combining (2) and (6) yields the prediction that the nucleation rate is proportional to the square of the equilibrium density:

$$\Gamma = \rho_k / \tau = \frac{4}{3b} D \alpha \rho_k^2, \quad (7)$$

The relation $\Gamma \propto \rho_k^2$ is also found in the discrete-space Ising model [18]. In contrast, the nucleation rate is proportional to ρ_k^3 in systems where nucleation does not occur in pairs [18,19]. The latter scaling was incorrectly predicted for the ϕ^4 system [8], from an estimate of the annihilation rate that does not take into account paired nucleation. (In the ϕ^4 system one does, however, find that the rate of survivor-survivor annihilation events – IV in Fig. 3 – is proportional to ρ_k^3 .) In the ϕ^4 SPDE, the parameters D , Γ and b have in general a weak (non-exponential) temperature dependence. The lengthscale b is of the same order as the width of an isolated kink.

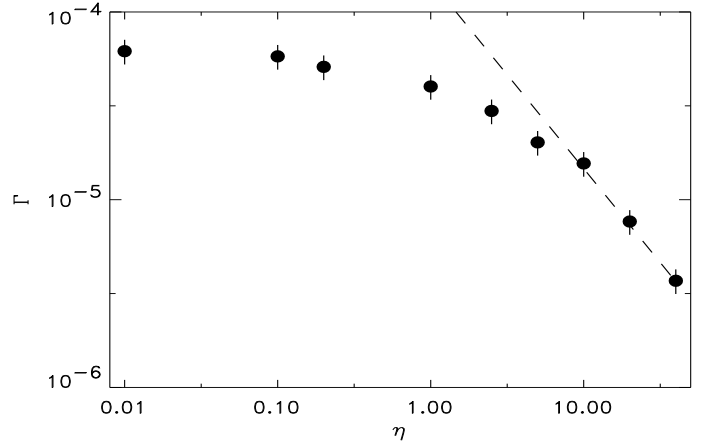


FIG. 5. Nucleation rate versus damping for $\beta = 6$. The dashed line has slope $1/\eta$.

In Fig. 5 we plot the measured nucleation rate versus the damping coefficient at fixed temperature. The nucleation rate is proportional to η^{-1} for $\eta \gg 1$ [in agreement with (7)] and appears to plateau for $\eta \rightarrow 0$. At low damping, however, direct measurement of the nucleation rate is problematic because kink-antikink collisions may result in single or multiple bounces rather than immediate annihilation [20].

We now turn to the lengthscales in the system. A histogram of distances between neighboring kinks and antikinks is well-approximated by an exponential with characteristic length $(2\rho_k)^{-1}$. This simple form results from the cancellation of the tendency of paired kinks to be closer together than $(2\rho_k)^{-1}$ with the opposite tendency of survivor kinks. In Fig. 6 we plot $f(x) = (\text{number of occurrences of separation} \in (x, x + dx)) / (L dx)$. We also construct the histogram for the separations of *only paired* kinks and antikinks. The dashed curve is the probability of being at x , averaged over the lifetime, for a Brownian motion killed at $x = 0$ and at rate μ [16]:

$$l(x) = N \exp(-\nu x) = N \exp(-\alpha \rho_k x). \quad (8)$$

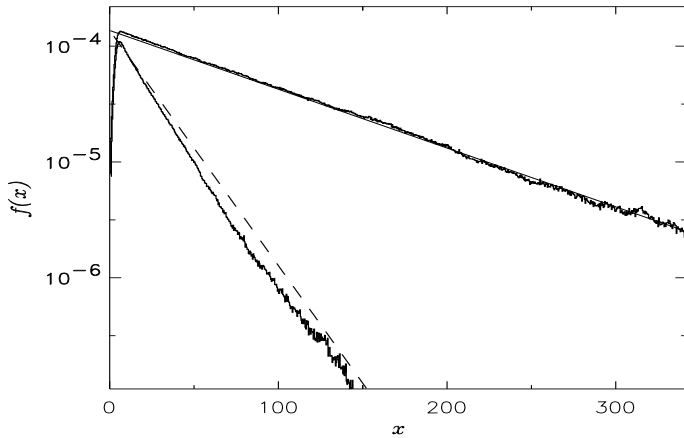


FIG. 6. Kink-antikink spacing. In the upper part of the plot, a histogram of all next-neighbor spacings is plotted with $(2\rho_k)^2 \exp(-2\rho_k x)$ (solid line). The lower part of the plot is a histogram of kink-antikink spacings only from paired kinks; the dashed line is $(2\rho_k)^2 \exp(-8\rho_k x)$. $\beta = 6$, $\eta = 1$.

The classification of kinks into paired kinks and survivors, with the approximation that kinks have a constant probability (2) per unit time of non-recombinant annihilation, allows us to construct a macroscopic rate theory for the two densities $n_p(t)$ (paired kinks) and $n_s(t)$ (survivor kinks). The equation for $n_p(t)$ has a positive term due to nucleation and a negative term inversely proportional to the lifetime of pairs, (4). The terms in the equation for $n_s(t)$ correspond to processes III and IV in Fig. 3. Note that process II does not change the number of survivor kinks. We obtain

$$\begin{aligned} \dot{n}_p &= \Gamma - 2b^{-1}\alpha D(n_s + n_p)n_p \\ \dot{n}_s &= D\alpha^2(n_s + n_p)^2(n_p - 2n_s). \end{aligned} \quad (9)$$

The steady state solution of (9) gives the relationship (7) between Γ and the equilibrium kink density. Nonequilibrium dynamics are also correctly described: if $\Gamma = 0$, the paired density quickly decays and, for late times, $\dot{n}_s \propto n_s^3$, in agreement with an exact result for the survival probability in the diffusion-limited reaction $A+A \rightarrow 0$ [21]. While not exact, (9) illustrate that at least two coupled equations are necessary to capture the two timescales in the dynamics: no single rate equation can suffice.

We have benefited from discussions with Kalvis Jansons, Eli Ben-Naim and Vincent Hakim. Computations were performed at the National Energy Research Scientific Computing Center (NERSC), Lawrence Berkeley National Laboratory.

[1] See, e.g., A. Seeger and P. Schiller, in *Physical Acoustics, Vol. III* edited by W.P. Mason (Academic, New York,

- 1966); A.R. Bishop, J.A. Krumhansl, and S.E. Trullinger, *Physica D* **1**, 44 (1980).
- [2] M. Peyrard and A.R. Bishop, *Phys. Rev. Lett.* **62**, 2755 (1989).
- [3] V.A. Kuzmin, V.A. Rubakov, and M.S. Shaposhnikov, *Phys. Lett.* **155B**, 36 (1985).
- [4] F.J. Alexander and S. Habib, *Phys. Rev. Lett.* **71**, 955 (1993); F.J. Alexander, S. Habib, and A. Kovner, *Phys. Rev. E* **48**, 4284 (1993).
- [5] S. Habib, A. Khare, and A. Saxena, *Physica D* **123**, 341 (1998); A. Khare, S. Habib, and A. Saxena, *Phys. Rev. Lett.* **79**, 3797 (1998).
- [6] L.M.A. Bettencourt, S. Habib, and G. Lythe, *Phys. Rev. D* (in press), hep-lat/9903007.
- [7] M. Buttiker and T. Christen, *Phys. Rev. Lett.* **75**, 1895 (1995); *ibid* **77**, 788 (1996); *Phys. Rev. E* **58**, 1533 (1998).
- [8] F. Marchesoni, *Phys. Rev. B* **34**, 6536 (1986); P. Hanggi, F. Marchesoni, and P. Sodano, *Phys. Rev. Lett.* **60**, 2563 (1988); F. Marchesoni, *ibid* **73**, 2394 (1994); P. Hanggi and F. Marchesoni, *ibid* **77**, 787 (1996); F. Marchesoni, C. Cattuto, and G. Constantini, *Phys. Rev. B* **57**, 7930 (1998).
- [9] D.J. Scalapino, M. Sears, and R.A. Ferrell, *Phys. Rev. B* **6**, 3409 (1972); J.A. Krumhansl and J.R. Schrieffer, *ibid* **11**, 3535 (1975); J.F. Currie, J.A. Krumhansl, A.R. Bishop, and S.E. Trullinger, *ibid* **22**, 477 (1980).
- [10] M. Buttiker and R. Landauer, *Phys. Rev. Lett.* **43**, 1453 (1979); *Phys. Rev. A* **23**, 1397 (1981).
- [11] R. Landauer and J.A. Swanson, *Phys. Rev.* **121**, 1668 (1961); A. Seeger and P. Schiller, in Ref. [1]; W. Wonneberger, *Physica A* **103**, 543 (1980).
- [12] A.I. Bochkarov and Ph. de Forcrand, *Phys. Rev. Lett.* **63**, 2337 (1989); *Phys. Rev. D* **47**, 3476 (1993); M. Alford, H. Feldman, and M. Gleiser, *Phys. Rev. Lett.* **68**, 1645 (1992).
- [13] T.R. Koehler, A.R. Bishop, J.A. Krumhansl, and J.R. Schrieffer, *Solid State Commun.* **17**, 1515 (1975); D.Yu. Grigoriev and V.A. Rubakov, *Nucl. Phys. B* **299**, 67 (1988).
- [14] T.R. Koehler *et al*, in Ref. [13]; W. Wonneberger, *Physica A* **108**, 257 (1981); D.J. Kaup, *Phys. Rev. B* **27**, 6787 (1983); Mario Salerno, E. Joergensen, and M.R. Samuelson, *Phys. Rev. B* **30**, 2635 (1984); P.J. Pascual and L. Vázquez, *Phys. Rev. B* **32**, 8305 (1985); F. Marchesoni, *Phys. Lett. A* **115**, 29 (1986).
- [15] I. Karatzas and S.E. Shreve, *Brownian Motion and Stochastic Calculus* (Springer, New York, 1988).
- [16] D. Dean and K.M. Jansons, *J. Stat. Phys.* **70**, 1313 (1993); K. Jansons and G. Lythe, *ibid* **90**, 227 (1998).
- [17] S. Habib, K. Lindenberg, G. Lythe and C. Molina-París, (in preparation).
- [18] Z. Rácz, *Phys. Rev. Lett.* **55**, 1707 (1985).
- [19] K. Lindenberg, P. Argyrakis, and R. Kopelman, *J. Phys. Chem.* **99**, 7542 (1995).
- [20] A.E. Kudryavtsev, *JETP Lett.* **22** 82 (1975); M. Moshir, *Nucl. Phys. B* **185**, 318, (1981); M.J. Ablowitz, M.D. Kruskal, and J.F. Ladik, *SIAM J. Appl. Math.* **36**, 428 (1979); D.K. Campbell, J.F. Schonfeld, and C.A. Wingate, *Physica D* **9**, 1 (1983).
- [21] D.C. Torney and H.M. McConnell, *J. Phys. Chem* **87**, 1941 (1983); D. Balding, *J. Appl. Prob.* **25**, 733 (1988).